Solution NMR Study of the Electronic and Molecular Structure of the Heme Cavity in High-Spin, Resting State Horseradish Peroxidase

Jeffrey S. de Ropp,[†] Pravat Mandal,[‡] Samuel L. Brauer,[‡] and Gerd N. La Mar*[,‡]

Contribution from the Department of Chemistry and the NMR Facility, University of California, Davis, California 95616

Received December 5, 1996[⊗]

Abstract: Three resting state horseradish peroxidase isozymes (HRP^C, HRP^{A1}, and HRP^{A2}) have been investigated by solution 1D and 2D NMR to determine the scope and limitation of these methods for large (∼44 kDa), high-spin ferric heme enzymes and to develop an interpretive basis of the hyperfine shifts in terms of the molecular and electronic structure of the active site. Definitive assignments are attained for the resolved heme and axial His resonances, as well as several residues more than 7 Å from the iron. Four Phe side chains located in HRP^C by scalar correlation and characteristic NOEs to the heme are identified as Phe 152, Phe 172, and two unassigned Phes X and W, in contact with pyrrole D. The temperature dependence of the hyperfine shifted aromatic rings shows that dipolar shift arises from zero-field splitting; a value of $D \sim 7$ cm^{-1} models the observed dipolar shift with use of a homology model constructed from peanut peroxidase. The combined use of steady-state NOEs, paramagnetic relaxation, and the predicted dipolar shifts based on the homology model led to the assignment of parts of the distal Arg 38 and Phe 41. However, the remainder of the active site signals are strongly relaxed but only weakly dipolar shifted, precluding assignment of other protons <7 Å from the iron. While the 1D/2D NMR approaches are not as effective in high-spin resting state HRP as for low-spin cyanide-inhibited HRP, several residues could be assigned in the former that were not located in the latter because both the residue and heme contact signals are lost under the diamagnetic envelope. With all heme signals resolved, HRP allows probing of the peripheral environment for all four pyrroles. Comparison of the hyperfine shift pattern among natural HRP isozymes reveals that the different shift magnitudes reflect variations in the extent of admixing of $S < {}^5/_2$ spin states to the predominant high-spin ground state. The binding of the substrate benzhydroxamic acid to HRP^C is shown to lead to altered hyperfine shifts that reflect an increase of the zero-field splitting and demonstrates that the binding of the substrate, in contrast to previous proposals, is not accompanied by ligation of a water at the sixth position. It is also concluded that the available methods are sufficient to allow definitive NMR studies of the peripheral substrate binding site in HRP.

Introduction

Horseradish peroxidase (HRP)[1] is a member of the large class of heme peroxidases which carry out one-electron oxidation of a variety of substrates at the expense of H_2O_2.[2] HRP has served a unique role in the understanding of enzyme reactions in general and, because of the lack of a crystal structure, a dominant role in the development of spectroscopic approaches to elucidate molecular and electronic structural properties relevant to function.[3−13] ^{1}H NMR spectroscopy has provided a wealth of such information.[4−13] The more favorable relaxation properties and large spectral dispersion due to large magnetic anisotropy of the low-spin, cyanide-inhibited ferric enzyme, HRP-CN, have provided by far the most extensive and detailed information on the active site,[5−7] but suffer from the disadvantage that this is not a physiologically relevant derivative. The model for HRP

[†] NMR Facility.

[‡] Department of Chemistry.

[⊗] Abstract published in *Advance ACS Abstracts,* May 1, 1997.

(1) Abbreviations used: ppm, parts per million; DSS, 2,2-dimethyl-2-silapentane-5-sulfonate; HRP, horseradish peroxidase; WEFT, water-eliminated Fourier transform; BHA, benzhydroxamic acid; NOESY, two-dimensional nuclear Overhauser spectroscopy; TOCSY, two-dimensional total correlation spectroscopy; PNP, peanut peroxidase; NOE, nuclear Overhauser effect; ZFS, zero-field splitting; metMb, ferric high-spin myoglobin.

(2) Dunford, H. B. *Peroxidases in Chemistry and Biology*; (Everse, S. L., Everse, K. E., Grisham, M. B., Eds.; CRC Press: Boca Raton, FL, 1991; Vol. II, pp 1−23. Ortiz de Montellano, P. R. *Annu. Rev. Pharmacol. Toxicol.* **1992**, *32*, 89−107. Poulos, T.; Fenna, R. E. *Metal Ions in Biological Systems*; Sigel, H., Sigel, A., Eds.; Dekker: New York, 1994; Vol. 30, pp 25−76.

(3) Spiro, T. G., Ed. *Biological Application of Raman Spectroscopy*; Wiley: New York, 1988; Vol. 3. Palmer, G. *The Porphyrins*; Dolphin, D., Ed.; Academic Press: New York, 1979, Vol. IVB, pp 313−353. Andersson, L. A.; Dawson, J. H. *Struct. Bonding* **1990**, *74*, 2−40. Bertini, I.; Turano, P.; Vila, A. J. *Chem. Rev.* **1993**, *93*, 2833−2932.

(4) Satterlee, J. D. *Annu. Rep. NMR Spectrosc.* **1986**, *17*, 79−178.

(5) Williams, R. J. P.; Wright, P. E.; Mazza, G.; Ricard, J. R. *Biochem. Biophys. Acta* **1975**, *412*, 127−147. Morishima, I.; Ogawa, S.; Inubushi, T.; Yonezawa, T.; Iizuka, T. *Biochemistry* **1977**, *16*, 5109−5115. de Ropp, J. S.; La Mar, G. N.; Smith, K. M.; Langry, K. C. *J. Am. Chem. Soc.* **1984**, *106*, 4438−4444. Banci, L.; Bertini, I.; Turano, P.; Ferrer, J. C.; Mauk, A. G. *Inorg. Chem.* **1991**, *30*, 4510−4516. Sette, M.; de Ropp, J. S.; Hernandez, G.; La Mar, G. N. *J. Am. Chem. Soc.* **1993**, *115*, 5237−5245. de Ropp, J. S.; Yu, L. P.; La Mar, G. N. *J. Biomol. NMR* **1991**, *1*, 175−190. Thanabal, V.; de Ropp, J. S.; La Mar, G. N. *J. Am. Chem. Soc.* **1987**, *109*, 265−272. Thanabal, V.; de Ropp, J. S.; La Mar, G. N. *J. Am. Chem. Soc.* **1988**, *110*, 3027−3035.

(6) Thanabal, V.; de Ropp, J. S.; La Mar G. N. *J. Am. Chem. Soc.* **1987**, *109*, 7516−7525.

(7) Chen, Z.; de Ropp, J. S.; Hernandez, G.; La Mar, G. N. *J. Am. Chem. Soc.* **1994,** *116*, 8772−8783.

(8) Morishima, I.; Ogawa, S. *J. Biol. Chem.* **1979**, *254*, 2814−2820.

(9) La Mar, G. N.; de Ropp, J. S.; Smith, K. M.; Langry, K. C. *J. Biol. Chem.* **1980**, *255*, 6646−6652.

(10) La Mar, G. N.; Thanabal, V.; Johnson, R. D.; Smith, K. M.; Parish, D. W. *J. Biol. Chem.* **1989**, *264*, 5428−5434.

(11) Thanabal, V.; de Ropp, J. S.; La Mar, G. N. *J. Am. Chem. Soc.* **1986**, *108*, 4244−4245. Thanabal, V.; La Mar, G. N.; de Ropp, J. S. *Biochemistry* **1988**, *27*, 5400−5407.

(12) La Mar, G. N.; de Ropp, J. S. *Biochem. Biophys Res. Commun.* **1979**, *90*, 36−41.

(13) de Ropp, J. S.; La Mar, G. N. *J. Am. Chem. Soc.* **1991**, *113*, 4348−4350.

S0002-7863(96)04201-1 CCC: $14.00

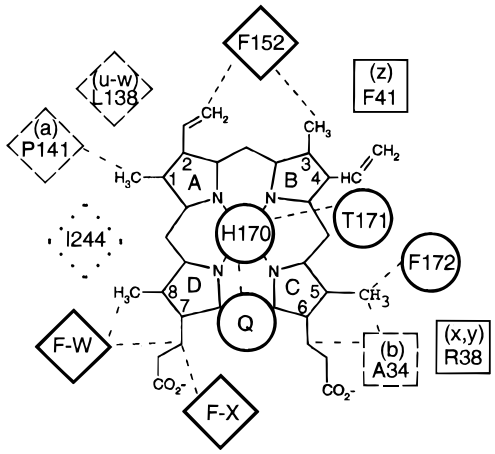

Figure 1. Residues in the heme pocket in HRP^C identified by ^{1}H NMR and a homology model based on PNP. Residues identified in both HRP^C and HRP^C-CN are shown by a dark solid border; those identified in both derivatives but without dipolar contacts to the heme in the resting state are shown by a light solid border; and those identified only in HRP^C are shown by a dashed border (the lower case letters identifying the relevant NMR signals are given in parentheses). I244 (dotted border) was located in HRP^C-CN but not HRP^C. Circles and squares reflect residues in the proximal and distal sides of the heme, respectively, with diamonds indicating heme peripheral residues. NOESY contacts observed in HRP^C are indicated by dashed lines.

derived from the NMR data[7] on HRP-CN is shown schematically in Figure 1.

NMR studies of the active site in resting state HRP[8−13] have been fewer and more limited in scope than those in the cyanide-inhibited complex. The resting state, HRP, because of its predominantly high-spin ferric ion,[14] leads to considerably stronger relaxation (by a factor of ∼10) and leads to large contact-dominated hyperfine shifts for the heme and axial His, and much smaller (relative to linewidth) dipolar shifts for nonligated residues.[8−13] Moreover, not only is intrinsic T_1 paramagnetic relaxation much stronger in HRP than HRP-CN, but the large size (∼44 kDa) and number of unpaired spins (5) of the former induces strong Curie relaxation,[15] which selectively decreases T_2 (increases linewidth) thereby largely canceling the advantages of high spectrometer field strength ($T_2^{-1} \propto B_o^2 R_{Fe}^{-6}$). Limited ^{1}H NMR studies on HRP have yielded only heme[9−11,13] and axial His[11,12] assignments with use of a combination of isotope labeling[9,10] and, more recently, 1D[6,11] and 2D[13] NMR methods. In this study we explore the scope and limitations of NMR methods[16] in defining the molecular and electronic structures of resting state HRP. This includes definitive assignments via scalar correlation of residues in the heme pocket and determination of their disposition relative to the heme by using both dipolar correlation and analysis of iron-induced dipolar shifts with the results on HRP-CN[7] as a reference.

The hyperfine shift, δ_{hf}, is the sum of the contact, δ_{con}, and dipolar, δ_{dip}, contributions:[4,17]

$$\delta_{hf} = \delta_{con} + \delta_{dip} \tag{1}$$

The former reflects Fe-ligand covalency and delocalized spin density, ρ ($A/\hbar \propto \rho$), via

$$\delta_{con} = -\frac{A}{\hbar}\frac{g\beta S(S+1)}{3kT\gamma} \tag{2}$$

Dipolar shifts in a $S > {}^1/_2$ ferric heme in the limit of axial symmetry are given by:[17]

$$\delta_{dip} = \left[\frac{S(S+1)\beta^2(g_{||}{}^2 - g_{\perp}{}^2)}{9kT} + \frac{S(S+1)(2S-1)(2S+3)\beta^2(g_{||}{}^2 + {}^1/_2 g_{\perp}{}^2)D}{135k^2T_2}\right]\left[\frac{1-3\cos^2\theta}{R^3}\right] \tag{3}$$

where θ is the angle between the H_i−Fe vector and the unique (or z) magnetic axis, R is the length of this vector, D is the zero-field splitting factor, $g_{||}$ and $g_{\perp}$ are the spectroscopic splitting factor parallel and perpendicular to the magnetic axis, β is the Bohr magneton, S is the unpaired spins, k is the Boltzmann factor, and T is absolute temperature. Inspection of eq 3 reveals that anisotropy in the **g** tensor (first term) leads to dipolar shifts with T^{-1}, while zero-field splitting (second term) yields shifts with T^{-2} temperature dependence. In favorable cases where one or the other term dominates, knowledge of D or **g** tensor anisotropy allows interpretation of dipolar shifts in terms of the geometry of the residue relative to the heme. Such recent studies on a small "model" protein, high-spin ferricytochrome c', have shown that the origin of the dipolar shifts can be established and subsequently used to probe molecular structure near the heme.[18] Perturbations of the heme environment due to changes in the polypeptide chain (*i.e.*, isozymes, mutants) or substrate binding would be expected to induce very different *patterns* in hyperfine shift changes if the magnitude of the contact vs the dipolar shifts is altered. A minor problem in quantitatively applying eq 3 to HRP is that the magnetic moment (5.2 μ_B) is less than the spin-only value for $S = {}^5/_2$ (5.92 μ_B),[14] indicating a moderate contribution from a $S < {}^5/_2$ (likely $S = {}^3/_2$) state. The well-behaved variable temperature behavior of the heme hyperfine shifts[9] dictates that this is more likely a quantum mechanical than a thermal mixture of spin states.[19]

In this report, we address the following questions: How effective are the available NMR methodologies for resonance assignment? Can we formulate an interpretive basis of the hyperfine shifts? How does the information content of resting state HRP compare with that of the cyanide-inhibited HRP? The developed methodologies and interpretive bases will be used subsequently to analyze the influence of substrate binding[8,20,21] on the abundant C isozyme (HRP^C) and to compare the electronic and molecular structures to that of two acidic isozymes,[22] A1 and A2, designated HRP^{A1} and HRP^{A2}, for which the complete sequence is available for the latter,[23] but only limited sequence data are available for the former.[24] The resulting NMR data will be interpreted by using both the NMR

(14) Schonbaum, G. R. *J. Biol. Chem.* **1973**, *248*, 502−511.
(15) Gueron, M. *J. Magn. Reson.* **1975**, *19*, 58−66. Vega, A. J.; Fiat, D. *Mol. Phys.* **1976**, *31*, 347−353.
(16) La Mar, G. N.; de Ropp, J. S. in *Biological Magnetic Resonance*; Berliner, L. J., Reuben, J., Eds.; Plenum Press: New York, 1993; Vol. 12, pp 1−73.
(17) Jesson, J. P. *NMR of Paramagnetic Molecules: Principles and Applications*; La Mar, G. N., Horrocks, W. D., Jr., Holm, R. H., Eds.; Academic Press: New York, 1973; pp 1−52.
(18) Clark, K.; Dugad, L. B.; Bartsch, R. G.; Cusanovich, M. A.; La Mar, G. N. *J. Am. Chem. Soc.* **1996**, *118*, 4654−4664.
(19) Maltempo, M. M.; Ohlsson, P. I.; Paul, K. G.; Petersson, L.; Ehrenberg, A. *Biochemistry* **1979**, *18*, 2935−2941.
(20) Sakurada, J.; Takahashi, S.; Hosoya, T. *J. Biol. Chem.* **1986**, *261*, 9657−9662.
(21) La Mar, G. N.; Hernandez, G.; de Ropp, J. S. *Biochemistry* **1992**, *31*, 9158−9168.
(22) Gonzalez-Vergara, E.; Meyer, M.; Goff, H. M. *Biochemistry* **1985**, *24*, 6561−6567.
(23) Welinder, K. G. *Plant Peroxidase 1980*−1990: Topics and Detailed Literature on Molecular, Biochemical, and Physiological Aspects; Penel, C., Gaspar, T., Greppin, H., Eds.; University of Geneva Press: Geneva, Switzerland, 1992; pp 1−24.
(24) Welinder, K. G. Private communication.

results on the cyanide-inhibited complex[7] and the recent crystal structure of a homologous class III peroxidase, peanut peroxidase,[25] PNP, as a homology model to evaluate the data.

Experimental Section

Proteins. Purified HRP isozyme C (HRP^C) was purchased from Boehringer-Mannheim; purified HRP acidic isozymes A1 (HRP^{A1}) and A2 (HRP^{A2}) were purchased from Sigma. All were obtained as lyophilized salt free powders and converted to 2−3 mM solutions in 99.96% ^2H_2O at pH 7.0 (not corrected for isotope effect).

NMR Spectra. ^{1}H NMR spectra were obtained on General Electric NMR Omega 300 MHz and Omega 500 MHz spectrometers. 1D and 2D spectra were obtained under a variety of conditions on both spectrometers; details of the data collection and processing parameters are included in the relevant figure captions. Dipolar correlations were obtained from NOESY[26] experiments with short mixing times of 3−20 ms; scalar correlation was determined by clean-TOCSY experiments to suppress ROESY-type responses.[27] Short TOCSY mixing times (9−20 ms) were used throughout to compensate for paramagnetic relaxation.[16] Steady-state NOEs over the temperature range 25−55 °C were obtained with a 30 ms irradiation time, utilizing 8 scans of saturation of the peak of interest followed by 8 scans with the irradiation frequency off-resonance with phase cycling of the receiver to generate a difference spectrum; line broadening of ∼30 Hz was used prior to Fourier transformation. Nonselective T_1s were measured by standard inversion−recovery methods. The relationship[4]

$$T_{1,2}{}^{A}/T_{1,2}{}^{B} = (R_{Fe-A})^6/(R_{Fe-B})^6 \quad (4)$$

was used to qualitatively estimate T_1 and line width values. The use of a heme methyl $T_1 \sim 9$ ms for $R_{Fe} = 6.1$ Å as a reference leads to a lower limit on R_{Fe-X} inasmuch as the heme methyl T_1 may reflect some dipolar relaxation by delocalized as well as iron unpaired spin density.[16] For T_2s (line width), eq 4 is approximate since only a portion of the line width arises from hyperfine relaxation. Chemical shifts were referenced to the solvent, which in turn had been calibrated to internal 2,2-dimethyl-2-silapentane-5-sulfonate (DSS).

Data sets were processed either on a SPARC II work station with GE-NMR Ω software, version 6.0, or on a Silicon Graphics Indigo-2 with the Biosym software FELIX, versions 2.30 and 95.0. TOCSY and NOESY data sets were processed with 30 to 60°-shifted sine-bell-squared apodization in both dimensions. All 2D data sets were zero-filled to 1024 × 1024 or 1024 × 2048 points. Data were phase-corrected and base-line leveled in both dimensions. Further details of data processing are included in the relevant figure captions.

Molecular Models. Replacement of amino acids in the PNP structure[25] and calculation of interatomic distances and angles were done by using the Insight II, version 95.0, software from Biosym. A simple homology model of HRP was constructed, replacing 18 residues (out of 63) within 12 Å of the iron in PNP. The resultant coordinates were used to calculate δ_{dip}(calc) values for the protons in the HRP model from eq 3. The total calculated shift

$$\delta_{DSS}(\text{calc/obs}) = \delta_{dia} + \delta_{dip}(\text{calc/obs}) \quad (5)$$

where δ_{dia} is the shift (including ring current and secondary structural contributions) expected for a diamagnetic analog,[28] which is calculated on the basis of the homology model.

Results

Comparison of Isozymes. The resolved portions of the 300-MHz ^{1}H NMR spectra under rapid repetition WEFT[29] conditions for resting state HRP^C, HRP^{A1}, and HRP^{A2} in ^2H_2O at pH 7.0 and 40 °C are shown in Figure 2. The previously reported assignments[9,10,12,13] for HRP^C are given, and the assignments determined herein for the acidic isozymes are shown by dashed line connections. The spectra for the acidic isozymes appear the same as those reported previously,[22] except for significantly improved sensitivity. An additional broad, single proton resonance is observed near 95 ppm for each isozyme (not shown, but listed in Table 1). The three isozymes exhibit low-field methyl peaks with similar line width, *i.e.* 300 ± 50 Hz for the resolved 5-CH_3, although the value for HRP^{A2} appears somewhat smaller than that for HRP^C. Nonselective T_1s at 40 °C yield 8 ± 2 ms for all heme α-substituents and 2 ± 1 ms for the axial His C_βHs. A very broad and strongly relaxed peak z on the upfield shoulder is observed optimally at 55° for HRP^C, as shown in Figure 2D.

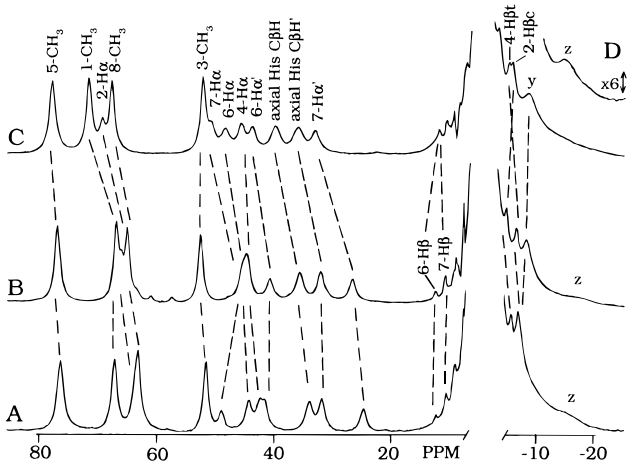

Figure 2. WEFT reference spectra of HRP isozymes at pH 7.0. Spectra A−C are portions of the spectra at 300 MHz, 40 °C, for (A) HRP^{A2}, (B) HRP^{A1} and (C) HRP^C. Spectrum D shows the upfield WEFT spectrum of HRP^C at 300 MHz, 55 °C, emphasizing the resolved peak z. Dotted lines connect assigned peaks in the three isozymes. Data were collected at a repetition rate of 40 s^{-1}, a sweep width of 200 ppm, and a relaxation delay of 10−14 ms and apodized with 30 Hz line broadening.

Table 1: Summary of Heme and Axial His Chemical Shifts (ppm) for Resting State HRP Isozymes[a]

	40 °C			55 °C	
resonance	HRP^{A1} [a]	HRP^{A2} [a]	HRP^C [a]	HRP^C [a]	BHA:HRP^C [a,b]
mean[c] heme CH_3	65.2	64.4	67.0	63.9	65.3
spread[d] heme CH_3	24.2	24.5	25.6	24.2	26.7
axial His $N_\delta H$	93.1	92.4	95.2	91.8	94.8
mean[e] axial His $C_\beta H$	34.0	32.8	37.7	36.4	34.0

[a] Chemical shift in ^2H_2O, pH 7.0, referenced to DSS. [b] Chemical shift with 3 equiv (saturating amount) of BHA. [c] Arithmetic mean of the four heme chemical shifts, $\bar{\delta}$(heme CH_3). [d] Maximum difference in heme methyl chemical shift. [e] Arithmetic mean of axial His $C_\beta H$ chemical shifts, $\bar{\delta}$(axial His C_βHs).

Heme Assignments. Heme assignments for all protons except the propionate H_βs and meso-Hs of HRP^C were obtained previously by isotope labeling[9] and steady-state NOEs[11] and subsequently shown to be obtainable by 2D NOESY spectra.[13] The observation of strong NOESY cross peaks for both propionate H_αs to a pair of geminal protons in the 7−12 ppm window locates the H_βs (not shown, see Supporting Information); the assignment is confirmed by the loss of these NOESY cross peaks in a sample reconstituted with heme deuterated at the propionate β position (not shown). The signals for the meso-Hs ($R_{Fe} \sim 4.4$ Å) are expected to exhibit line widths >2 kHz and $T_1 < 1$ ms, and are not detected by ^{1}H NMR. They have

(25) Schuller, D. J.; Ban, N.; van Huystee, R. B.; McPherson, A.; Poulos, T. L. *Structure* **1996**, *4*, 311−321.
(26) Macura, S.; Ernst, R. R. *Mol. Phys.* **1980**, *41*, 95−117.
(27) Griesinger, C.; Otting, G.; Wüthrich, K.; Ernst, R. R. *J. Am. Chem. Soc.* **1988**, *110*, 7870−7872.
(28) Cross, K. J.; Wright, P. E. *J. Magn. Reson.* **1985**, *64*, 220−231. Wishart, D. S.; Sykes, B. D.; Richards, F. M. *J. Mol. Biol.* **1991**, *222*, 311−333.
(29) Patt, S. L.; Sykes, B. D. *J. Chem. Phys.* **1972**, *56*, 3182−3184.

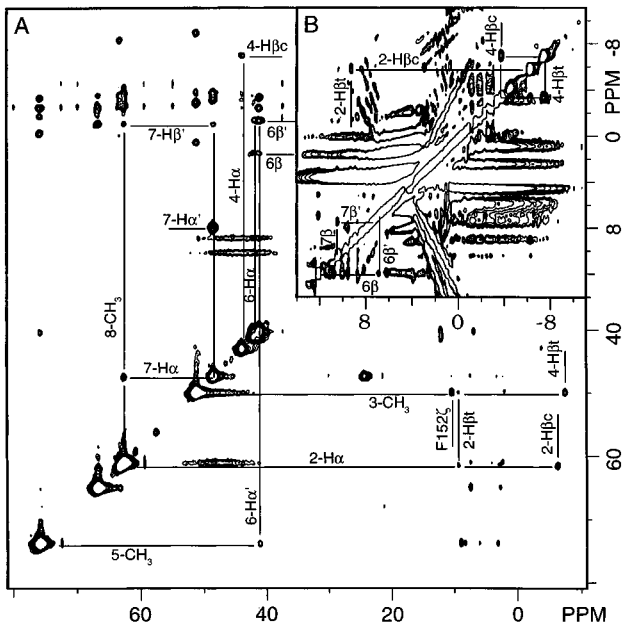

Figure 3. 300-MHz NOESY spectrum of HRP^{A2} in ^2H_2O, at pH 7.0 and 40 °C, obtained with a mixing time of 8 ms over a 200 ppm band width to emphasize hyperfine shifted peaks. Panels A and B are the same data set but processed differently: (A) data processed with 60°-shifted sine-bell-squared apodization to favor broad lines and (B) the expansion processed with 30°-shifted sine-bell-squared apodization to increase resolution near the diamagnetic window. Recycle time of the pulse sequence was 50 ms, and the overall data collection time was 42 h with 6080 scans/block.

been located and assigned under the diamagnetic envelope by direct ^2H NMR detection of a suitably labeled protein.[10]

The NOESY map for $\tau_m = 8$ ms for HRP^{A2} in ^2H_2O is illustrated in Figure 3 and provides, upon comparison with the NOESY map for HRP^C, all of the cross peaks to assign the complete heme except the meso-Hs. A similar map provided these assignments for HRP^{A1} (not shown). The pattern of shifts around the heme is strongly conserved among the three isozymes except for small changes of the mean methyl shifts, $\bar{\delta}$(heme CH_3), as given in Table 1. The individual shifts of all assigned heme signals for the three isozymes are listed in Supporting Information.

Axial His. The His 170 C_βHs have been sequence-specifically assigned[7] in HRP^C-CN, and saturation transfer[6] from the remaining two resolved non-heme, low-field peaks in HRP^C (Figure 2C) definitively assigned them in the resting state. The His 170 C_βHs exhibit very short T_1s (vide supra), and on this basis the two remaining non-heme rapidly relaxing downfield peaks in both HRP^{A1} and HRP^{A2} can be assigned to the axial His in each isozyme. The broad low-field peak (∼95 ppm) present in ^2H_2O has been shown to arise from the axial His 170 in HRP^C, which exhibits extraordinarily slow exchange with solvent.[12] Similar resonances are observed for the acidic isozymes (Table 1). From eq 4 the His 170 ring CHs ($R_{Fe} \sim$ 3.4 Å) would exhibit line widths >10 kHz and T_1s < 0.1 ms, and are not detected by ^1H NMR. The axial His $N_\delta H$ and mean $C_\beta H$ shift, $\bar{\delta}$(axial His C_βHs), for the three isozymes are included in Table 1 and the individual shifts listed in Supporting Information.

Residues with Aromatic Rings. These residues take a special place in the analysis of high-spin ferric hemoproteins since their diamagnetic chemical shifts are well defined (∼7 ppm), there are only relatively few (compared to aliphatic) such residues in HRP, and the Phe ring spin systems can be clearly defined in TOCSY spectra. The temperature response of the necessarily dipolar shifts for such aromatic rings reveals the mechanism[17,18] of the dipolar shift (zero-field splitting *vs* **g**-tensor anisotropy in eq 3). Three Phe rings in contact with the heme have been clearly identified[7] for HRP^C-CN: Phe 152 in contact with 3-CH_3, Phe 172 in contact with 5-CH_3, and the unassigned Phe W near 8-CH_3. A fourth Phe (Phe X) was tentatively assigned[7] in HRP^C-CN with apparent contact with the 7-propionate H_α. As conditions for definitive assignments, we demand the detection of NOEs from the heme to at least two of the spin-coupled aromatic ring protons, which in turn can be connected by TOCSY cross peaks and/or the detection of NOEs to an aromatic proton with significant dipolar shifts for which the contact can be observed over a range of temperatures. NOESY cross peaks from the respective heme signals to the aromatic window can be identified in the 2D maps for resting state HRP^C, but the wide band width and low resolution of the 2D maps are insufficient for assignment. Instead, we rely on steady-state NOEs, saturating the individual heme substituent peaks and analyzing the difference spectra for resonances which, in turn, exhibit cross peaks in NOESY and TOCSY maps collected over only the diamagnetic envelope (with much higher resolution).

The NOE difference traces in the 11 to 5 ppm window for the relevant heme side chains are shown in Figure 4, spectra A−D, and the appropriate NOEs to Phes 152, 172, W, and X are present. The chemical shifts and intercepts at infinite temperatures for plots of chemical shift versus T^{-1} and T^{-2} ($\delta_{int}(T^{-1})$, $\delta_{int}(T^{-2})$) are listed in Table 2. It is clear that the expected intercepts of ∼7 ppm are observed for $\delta_{int}(T^{-2})$, but not for $\delta_{int}(T^{-1})$. When these steady-state NOEs are compared to a short mixing time (12 ms) TOCSY spectrum (Figure 4E), the complete rotationally averaged spin systems for three Phe side chains are located; the putative Phe X exhibits only one TOCSY cross peak. The chemical shift of each NOE-detected peak as a function of temperature correlates with the cross peak positions in the TOCSY map at different temperatures (not shown). For Phe X, the positions of neither the NOE nor the one TOCSY peak are significantly affected by temperature, hence, the NOE/TOCSY data are consistent with, but not proved for, a Phe X in contact with 7H_α. The NOE contacts with the heme are shown schematically in Figure 1. Other NOEs detected to protons with chemical shifts in the aromatic spectral window invariably exhibit temperature dependence that yields intercepts in the aliphatic window and, with few exceptions, are not considered further.

Similar steady-state NOE studies were conducted on the acidic isozymes, and irradiation of 3-CH_3 and 5-CH_3 identifies the homologs of F152, F172 in both HRP^{A1} and HRP^{A2} (see Supporting Information), as predicted[23] by sequence data for HRP^{A2}. Irradiation of 8-CH_3 in both acidic isozymes (see Supporting Information) confirms that Phe W is absent in both HRP^{A1} and HRP^{A2}, consistent with observations on the low-spin CN derivative.[7,30] From inspection of the homology model the NOE contacts of Phe W to 8-CH_3 and Phe X to 7-H_α are most consistent with Phe W = Phe 179 and Phe X = Phe 221. The coordinates Phe 179 and Phe 221 were accordingly used to obtain δ_{dip}(calc) and δ_{DSS}(calc) in Table 2; the values of observed and calculated shifts agree well for Phe W but less so for Phe X.

Interpretative Basis of Dipolar Shifts. The intercepts at infinite temperature in plots of shift versus T^{-2} for the four Phe rings clearly indicate that the dipolar shifts arise primarily from

(30) de Ropp, J. S.; Chen, Z.; La Mar, G. N. *Biochemistry* **1995**, *34*, 13477−13484.

(31) Mandal, P.; de Ropp, J. S.; La Mar, G. N. Manuscript in preparation.

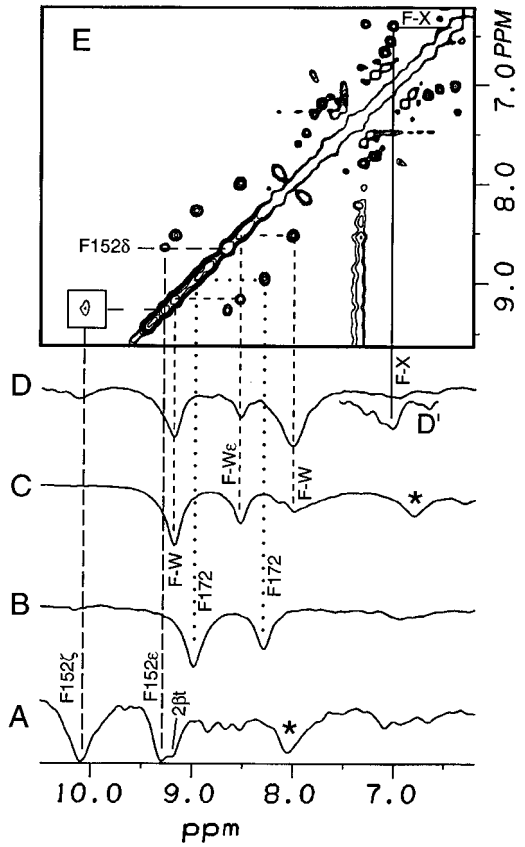

Figure 4. 500-MHz one-dimensional NOE difference spectra and TOCSY spectrum of the aromatic region of HRP^{C} at 55 °C and pH 7.0. 1D traces show NOE difference spectra for irradiation of heme (A) 3-CH_3, (B) 5-CH_3, (C) 8-CH_3, and (D) 7$_\alpha$H; panel E is a 12 ms mixing time TOCSY spectrum. Intraresidue connectivities are shown for (− −) Phe 152, (···) for Phe 172, (- - -) Phe W, and (—) Phe X (an NOE is also present from 2-H$_{\beta c}$ to Phe 152, not shown). The boxed insert to panel E shows a F152 cross peak obtained at a lower contour level. NOE difference spectra were collected with a 30 ms irradiation time, a 200 ppm sweep width, and a recycle rate of 20 s^{-1}. Data were processed with zero filling to 8192 points and 30-Hz apodization. TOCSY data were collected with a 12 ms mixing time to assist cross peak detection for rapidly relaxed peaks, using a 20 ppm sweep width and a recycle rate of 5 s^{-1}. Unassigned NOEs in the aromatic spectral window marked with an asterisk have T^{-2} intercepts in the aliphatic region.

zero-field splitting, ZFS, and that the magnitude of the shifts, together with the PNP crystal structure,[25] can be used to estimate D in eq 3. Assuming that the zero-field splitting term is axially symmetric and essentially normal to the heme, δ_{dip}(obs) in Table 2, obtained via eq 5 for the conserved Phe 152 and Phe 172, agrees well with δ_{dip}(calc) by using $D \sim 7$ cm^{-1} for $S = {}^5/_2$ (however, see Discussion), a value similar to that determined for other high-spin ferric hemoproteins.[32−34]

At this point, we pursue less direct assignments where the NMR data are used in parallel with the predictions of the homology model, using the second term in eq 3 with $D = 7$ cm^{-1} and $S = {}^5/_2$ and predicted lower limits to T_1s from eq 4 using $T_1 \sim 9$ ms (at 55 °C) for a heme methyl ($R_{Fe} = 6.1$ Å). δ_{dip}(calc) and δ_{DSS}(calc), obtained via eqs 3 and 5 from the homology model for the key active site residues Arg 38, Phe 41, His 42, and Ile 244 previously identified[7] in HRP-CN, predict that only three signals on these residues will resonate outside the intense 10 to −1 ppm diamagnetic envelope (Arg 38 C$_{\gamma 1}$H, C$_{\gamma 2}$H at −10.2, −3.9 ppm, Phe 41 C$_\epsilon$Hs at −2.2 ppm (Table 2); other shifts are listed in Supporting Information).

Other Resolved Residues. Two strongly relaxed and hyperfine shifted peaks labeled y and z (Figure 2, spectra C and D, and Table 2) are observed upfield with T_1s of ∼2 and 1 ms, respectively. The prediction of the homology model leads to shifts that will result in strongly upfield resolved resonances only for the CγHs of Arg 38 and Phe 41 C$_\epsilon$Hs (see above and Supporting Information). In HRP^{C}, the large line widths of these resonances precluded steady-state NOE measurements. However, in HRP^{A1} (where these resonance line widths are narrower) irradiation of y produced a strong NOE appropriate only for a geminal partner to a broad peak labeled x under the intense composite at −3.1 ppm on the upfield shoulder (Figure 5). The only proton sufficiently close to the iron with a geminal partner in HRP-CN is Arg 38 C$_{\gamma 1}$H. The large apparent NOE (∼25%) is consistent with a geminal partner for the predicted T_1 of C$_{\gamma 2}$H of Arg 38. We tentatively assign a similarly shifted and relaxed proton in HRP^{C} as x (Table 2) and ascribe x and y to the geminal Arg 38 CγH protons. The only other signal predicted to be well resolved is that for the averaged H$_\epsilon$s of the Phe 41 ring, but the δ_{dip}(calc) = −5.7 ppm yields a δ_{DSS}(calc) well to the low-field side of peak z in Table 2. However, a small change in the orientation of Phe 41 by as little as ∼0.5 Å leads to δ_{dip}(calc) and δ_{DSS}(calc) of −13 and −9 ppm, respectively, which is in better agreement with the observation for peak z. The estimated T_1 for peak z in Table 2 is also within the bounds obtained by eq 4 in the homology model for Phe 41 C$_\epsilon$Hs; we propose that peak z arises from Phe 41 C$_\epsilon$Hs.

Two methyl peaks v and w and single proton peak u with only moderate relaxation and upfield dipolar shifts are observed on the upfield shoulder, as shown in Figure 6A and Table 2. Short mixing time TOCSY (Figure 6B) shows that the methyl peaks v and w are part of an isopropyl fragment, and further extend the correlation from the single C$_\gamma$H proton to a relaxed and upfield dipolar shifted methylene group (C$_\beta$H$_2$) that includes peak u. This establishes that the residue is Leu rather than Val. The observed relaxivity, upfield dipolar shifts, and sequence homology with PNP dictate that the origin of peaks u, v, and w is Leu 138; the predicted dipolar shifts are in good agreement with the observed values (Table 2). This assignment is further corroborated by comparison with HRP^{A1}, which also has Leu at this position[24] and shows a similar TOCSY pattern of two upfield CH_3 groups both spin coupled to the same proton (not shown; see Supporting Information). Altered chemical shifts and TOCSY/NOESY patterns for HRP^{A2} (not shown; see Supporting Information) are consistent with the known substitution Leu 138→Ile in this isozyme.[23] It is noteworthy that this homology model does not predict, nor are there observed (Tables 1, 2), any other dipolar shifted resonances which would resonate clearly outside the intense diamagnetic envelope. We do not observe the far (> −40 ppm) upfield peak previously reported.[22]

Other Nonresolved Residues. Two particularly intense NOEs are observed upon saturating the heme 1-CH_3 (to peak a, 7.8 ppm; Figure 7A) and the 5-CH_3 (to peak b, 3.1 ppm; Figure 7B). The 3.1-ppm NOE from 5-CH_3 is also present when the 6-H$_\alpha$ is irradiated, as shown in Figure 7C. Inspection of the homology model indicates that the contacts to 1-CH_3 and both 5-CH_3 and 6-H$_\alpha$ are the conserved Pro 141 C$_\alpha$H and Ala 34 C$_\beta$H$_3$, respectively; the experimental $\delta_{int}(T^{-2})$ for these protons are consistent with these assignments. The Pro 141 C$_\alpha$H shows TOCSY and NOESY cross peaks to two additional resonances which produce strong (geminal) NOESY/TOCSY

(32) Brackett, G. C.; Richards, D. L.; Caughey, W. S. *J. Chem. Phys.* **1971**, *54*, 4383−4401.
(33) Kao, Y.-H.; Lecomte, J. T. J. *J. Am. Chem. Soc.* **1993**, *115*, 9754−9762.
(34) Rajarathnam, K.; La Mar, G. N.; Chiu, M. L.; Sligar, S. G.; Singh, J. P.; Smith, K. M. *J. Am. Chem. Soc.* **1991**, *113*, 7886−7892.

Table 2: ^{1}H NMR data for dipolar shifted heme pocket residues of HRP^c at 55 °C, pH 7.0

		δ (ppm)						T_1 (ms)	
peak	assignment	$\delta_{DSS(obs)}$[a]	$\delta_{int}(T^{-1})$[b]	$\delta_{int}(T^{-2})$[c]	δ_{dip}(obs)[d]	δ_{dip}(calc)[e]	$\delta_{DSS(calc)}$[f]	$T_{1(calc)}$[g]	$T_{1(obs)}$[h]
	F152 ζ	10.08	4.0	7.2	2.1	2.2	10.2	16	21
	ϵ	9.20	3.5	6.5	1.4	1.2	9.0	44	
	δ	8.63	7.0	7.9	1.0	0.6	8.2	220	
	F172 ζ (or δ)[i]	8.97	1.4	7.3	0.9	1.2	9.2	52	
	ϵ	8.25	5.7	6.9	0.6	0.7	8.4	16	
	δ (or ζ)					−0.1	7.2	40	
	F-W ζ	8.01	6.6	8.0	0.4	0.5	8.1	160	
	ϵ	8.54	7.0	7.8	0.9	0.6	8.3	83	
	δ	9.15	5.2	6.7	1.4	1.0	8.7	62	
	F-X ζ (or δ)[i]	6.98	6.8	6.9	1.9	1.5	6.5	1	
	ϵ	6.38	6.4	6.5	−0.1	−0.9	5.6	4	
	δ (or ζ)					−1.9	4.7	20	
b	A34 $C_\beta H_3$	3.10	−0.1	1.3	1.8	0.9	2.2	87	
x	R38$C_{\gamma 2}$H (?)[j]	−3.23	12.7	4.3	−3.0	−3.6	−3.9	7	6
y	R38$C_{\gamma 1}$H (?)	−8.34	5.6	−1.9	−5.7	−7.6	−10.2	1	2
z	F41C_ϵHs (?)	−15.2			−11.3	−5.7	−2.2	1	1
	L138 C_αH	3.28			−0.8	−0.9	3.2	113	
	L138 $C_{\beta 2}$H	0.55			−0.7	−1.0	0.3	205	
u	L138 $C_{\beta 1}$H	−1.51	3.1	0.7	−2.4	−1.7	−0.8	66	38
	L138 C_γH	0.20			−1.0	−1.0	0.2	280	
v	L138 $C_{\delta 1}H_3$	−2.16	2.1	−0.1	−2.4	−1.3	−1.1	180	60
w	L138 $C_{\delta 2}H_3$	−2.50	1.2	−0.6	−2.2	−1.8	−2.1	83	45
a	P141 C_αH (?)	7.83	3.3	6.1	2.8	1.7	6.8	34	
	P141 $C_{\beta 1}$H (?)	3.68			0.7	2.0	5.0	26	
	P141 $C_{\beta 2}$H (?)	2.89			0.3	1.0	3.6	88	
	T171 NH	7.30			0.0	−1.4	5.9	51	

[a] Observed chemical shift in ppm, referenced to DSS. [b] Extrapolated intercept at T $\rightarrow \infty$, in ppm, of plot of observed chemical shift vs $1/T$. [c] Extrapolated intercept at T $\rightarrow \infty$, in ppm, of plot of observed chemical shift vs $1/T^2$. [d] Observed dipolar shift, in ppm, calculated via eq 5 from δ_{DSS}(obs) and δ_{dia}(calc). [e] Calculated dipolar shift, in ppm, from eq 3 with $S = {}^5/_2$ and $D = 7$ cm^{-1}. [f] Calculated total shift, in ppm, from eq 5.[g] T_1 value calculated from the iron-to-proton distance in the homology model and measured T_1 of 3-CH_3 resonance in HRP^C (9 ms at 55 °C, 500 MHz) with use of eq 4, and assuming dipolar relaxation solely by the iron. T_1s of ring proton pairs a,b calculated by using a weighted average distance from the iron, $R_{avg} = [0.5(R_a^{-6} + R_b^{-6})]^{-1/6}$. [h] T_1 measured from inversion−recovery data at 55 °C, pH 7.0, for resolved resonances at 500 MHz. [i] The ζ proton gives better δ_{DSS}(calc) than the δ proton, but latter cannot be excluded. [j] The question mark in parentheses indicates tentative assignments.

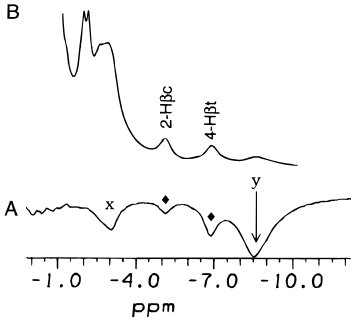

Figure 5. (A) Upfield portion of the 500-MHz steady-state NOE difference spectrum of HRP^{A1} at pH 7.0 and 45 °C, showing irradiation of peak y. A strong NOE is detected to peak x; the $2H_{\beta t}$ and $4H_{\beta c}$ peaks exhibit off-resonance saturation marked by closed diamonds. (B) WEFT reference trace for the upfield region of HRP^{A1} at pH 7.0 and 45 °C.

peaks (not shown), and these assign the Pro 141 C_βHs. Figure 7D shows NOEs observed for irradiation of the proximal His 170 C_βH proton (Table 1). A distinctive set of four upfield NOEs to an unidentified residue Q (first noted[7] in HRP^C-CN) are labeled q_1−q_4; the low-field NOE is to the Thr 171 NH[7] (Figure 7D). The upfield bias of the Q signals is consistent with the homology model, but the present data do not shed further insight into the nature of the residue Q side chain.

Influence of BHA. As reported previously,[8,20,21] titration of HRP^C with BHA leads to perturbations of all resonance positions up to addition of a molar equivalent. Some resonances broaden and shift with BHA and are indicative of small shift changes that fall in the intermediate to fast exchange region. Other resonances with large shift changes fall into the slow exchange region[21] and require assignments solely within the BHA:HRP^C complex. A 10 ms mixing time NOESY spectrum of BHA:HRP^C at 55 °C (not shown; see Supporting Material) yields the heme assignments in BHA:HRP^C at 55 °C with $\bar{\delta}$(heme CH_3) and $\bar{\delta}$(axial His C_βHs) as listed in Table 1, which then can be compared with the values for HRP^C at 55 °C. The changes in shifts are slightly smaller than those observed among the three isozymes.

Discussion

Effectiveness of 1D/2D NMR. The strong paramagnetic relaxation and small dispersion by the hyperfine fields clearly limit the scope of 1D/2D ^{1}H NMR investigation of high-spin relative to low-spin ferric hemoproteins. This is particularly true of large proteins like HRP (44 kDa) when compared to small proteins[18] like ferricytochrome c' (13 kDa), because of the adverse effect of Curie relaxation.[15] Hence the non-ligated residues in the immediate proximity of the heme cannot be identified unambiguously, and in HRP this includes the key catalytic residues Arg 38 and His 42. The difficulty in locating and assigning these residues is emphasized by the fact that the dipolar shift analysis of assigned residues places all but three protons for these residues under the diamagnetic envelope. Inasmuch as both T_1 and T_2 are a factor of ∼10 shorter in HRP than HRP-CN, the signal-to-noise for steady-state NOEs from the heme to Arg 38, Phe 41, and Ile 244 is reduced by $\sim 10^2$ in HRP relative to HRP-CN. However, some assignments are

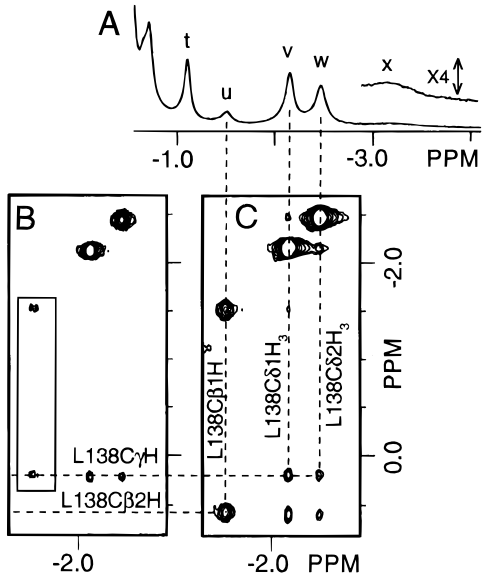

Figure 6. Portions of the 500-MHz ^{1}H NMR reference spectrum (A), TOCSY spectrum with $\tau_m = 12$ ms (B), and NOESY spectrum with $\tau_m = 20$ ms (C) for HRP^C in ^2H_2O at pH 7.0 and 55 °C, which provide definitive identification of a Leu (Leu 138) side chain with upfield dipolar shifts and moderate relaxation. Both 2D data sets were collected over a 30 ppm sweep width with a 5 s^{-1} repetition rate, with 256 complex points in t_1 and 1024 complex points in t_2 using 512 (TOCSY) or 640 (NOESY) scans per increment. Data were processed with 45°-shifted sine-bell-squared apodization in both dimensions and zero-filled in t_1 to 1024 points. The boxed insert to part B was plotted at a lower contour level.

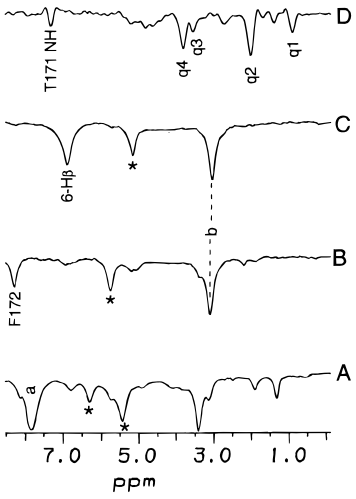

Figure 7. 500-MHz steady-state NOE difference spectra of HRP^C at 55 °C and pH 7.0 for irradiation of (A) 1-CH_3, (B) 5-CH_3, (C) 6$_\alpha$H, and (D) H170 C$_\beta$H. Data were collected with a 30 ms irradiation time, a 200 ppm sweep width, and a recycle rate of 20 s^{-1}. Data were processed with zero-filling to 8192 points and 30-Hz apodization. Assignments are labeled on the figure and discussed in the text. Unassigned low-field NOEs labeled by an asterisk all have intercepts ($\delta_{int}(T^{-2})$) in the aliphatic region (0−5 ppm), as do the peaks q_1−q_4.

attainable more readily in HRP than HRP-CN. Figure 1 shows that, of the 10 heme cavity residues previously identified in HRP^C-CN, six can be definitively identified in HRP^C, and some evidence for the presence of two (Arg 38 and Phe 41) can be inferred. The observed heme pocket contacts confirm a conserved structure for these residues in HRP^C and HRP^C-CN. Conversely, one residue, Leu 138, is identified only in HRP^C, and the presence of two others, Ala 34 and Pro 141, is inferred from the homology model and NOE pattern, but they have not been identified in HRP^C-CN. The detection of Pro 141 and Ala 34 candidates in HRP^C but not in HRP^C-CN is due to the fact that the heme 1-CH_3 and 5-CH_3 are not resolved in the latter derivative,[7] and hence such assignments are invariably more difficult. The readily identified peripheral aromatic residues in HRP^C have been postulated to play a major role in substrate binding,[30] in particular the ones close to 8-CH_3 (Phe W) and 7H$_\alpha$ (Phe X). Hence substrate binding studies[31] can be expected to be pursued as effectively in HRP as in HRP-CN.

The observed dipolar shifts for HRP are shown to result from magnetic anisotropy due to zero-field splitting rather than due to the **g**-tensor, and this allows the dipolar shift to be analyzed in terms of proton disposition relative to the heme normal,[18] inasmuch as ZFS is largely axial and perpendicular to the heme plane.[32−34] The value of $D \sim 7$ cm^{-1} is comparable to that reported for a variety of heme proteins[32−34] but closer to that for a six- rather than five-coordinate iron.[34,35] However, this value of D resulted from using the pure high-spin $S = {}^5/_2$ in eq 3. If the value of $S = 2.16$ obtained from the magnetic susceptibility data (5.2 μ_B)[14] is used in eq 3 then the value of D is 12 cm^{-1}, which is much closer to known values for five-coordinate hemoproteins.[34] Either set of magnetic moments and D values predicts dipolar shifts for the heme methyls and axial His C$_\beta$Hs of +3.4 and −6.2 ppm, respectively, which together with eqs 1 and 5 yields mean contact shifts of +58 and +42 ppm, respectively. It is therefore clear that the contact interaction strongly dominates both the heme and axial His hyperfine shift.

Comparison among HRP Isozymes. The pattern of heme, axial His and other hyperfine shifted resonances are very similar among the three HRP isozymes (Table 1 and Supporting Information), and confirm very similar molecular and electronic structures, as previously found for the cyanide-inhibited derivatives.[30] However, inspection of Table 1 reveals small, but systematic variations in shifts. The influence of the polypeptide chain on the heme cavity in the three isozymes is observed in a monotonic small increase in the mean hyperfine shifts for both the heme methyls (*i.e.*, δ(heme CH_3)) and axial His H$_\beta$ (*i.e.*, $\bar{\delta}$(axial His C$_\beta$Hs)), in the order HRP^{A2} < HRP^{A1} < HRP^C (Table 1). These changes clearly indicate that primarily the contact contribution to the shift increases in the same order, since a change primarily in the dipolar contribution would necessarily induce shifts for heme CH_3 and axial His C$_\beta$Hs in *opposite directions* due to the geometric factor eq 3. The increased contact shifts likely reflect changes in the effective S in eq 2, so that the degree of $S < {}^5/_2$ (likely $S = {}^3/_2$) ad-mixture in the ground spin state is largest for HRP^{A2} and smallest for HRP^C. While changes in the Fe-heme and Fe-His covalency (A/h in eq 2) cannot be ruled out as the origin of the shift changes, there is no reason to expect both the axial and equatorial bonds to be simultaneously more covalent. These two effects cannot be clearly distinguished in the absence of accurate magnetic susceptibility data for each of the three isozymes.

Influence of Substrate Binding. The influence of BHA on the mean heme methyl and the mean axial His H$_\beta$ shift in Table 1 is comparable in magnitude to that found among the three isozymes, but the shift *changes* are in the *opposite direction*, heme methyl shifts *increase* by 1.4 ppm and His C$_\beta$H shifts *decrease* by 2.4 ppm upon BHA binding. This ratio of heme methyl to axial His C$_\beta$H shift changes, −1.7, is virtually equal to the ratio of their calculated geometric factors in eq 3, −1.8, and hence dictates that primarily the dipolar shift (rather than

(35) Walker, F. A.; La Mar, G . N. *Annu. N.Y. Acad. Sci.* **1973**, *206*, 328−348.

S or covalency) *increases* upon BHA addition. Small 0.1−0.2 ppm larger low-field shifts for Phe 152, Phe 172, and Phe W and a 0.3−0.6 upfield shift for Leu 138 signals upon BHA binding (not shown) are also qualitatively consistent with the prediction of the increased dipolar shift. Hence, the major impact of BHA binding is an increase in the value of *D*. Resonance Raman studies have proposed[36] that BHA binding converts the iron from a penta- to a hexa-coordinated form, presumably via the ligation of a water molecule. Since it is known that the magnitude in *D decreases* with increased axial field strength in ferric hemes,[35] our NMR data argue strongly *against water ligation accompanying BHA binding*. This conclusion is supported by both ^{1}H NMR[33,34] and crystallographic[37] characterization of five- and six-coordinated heme iron metMb complexes. The conversion of five-coordinate metMb to six-coordinate metMbH_2O leads to *decreased* hyperfine shifts for both the heme methyls and axial His, as expected by the *trans* effect,[38] and is confirmed by smaller dipolar shifts for non-ligated residues in the six- than five-coordinate form.[34]

The nature of the modulation of the *D* value upon BHA binding is unclear at this time. It is noted, however, that BHA binding has a definite and select influence on the 6-propionate group, where it significantly increases the difference between the two 6-H_α hyperfine shifts (41.6 and 46.1 ppm for HRP^C at 55 °C) upon BHA binding (38.9 and 55.0 ppm for BHA:HRP^C at 55 °C; Supporting Information). This change in the contact contribution is indicative of a change in propionate orientation. The 6-propionate group has been shown to be in contact with the catalytically relevant Arg 38 side chain that extends over the heme surface.[7] Unfortunately, the response of the 6-propionate and Arg 38 to BHA binding cannot be probed further in the resting state enzyme. Such studies are in progress on the spectroscopically more tractable HRP^C-CN complex with and without BHA.

(36) Smulevich, G.; English, A. M.; Mantini, A. R.; Marzocchi, M. P. *J. Am. Chem. Soc.* **1991**, *30*, 772−779.

(37) Takano, T. *J. Mol. Biol*, **1977**, *110*, 569−584. Bolognesi, M.; Onesti, S.; Gatti, G.; Coda, A.; Ascenzi, P.; Brunori, M. *J. Mol. Biol.* **1989**, *205*, 529−544. Quillin, M. L.; Arduini, R. M.; Olson, J. S.; Phillips, G. N., Jr. *J. Mol. Biol.* **1993**, *234*, 140−155.

(38) Buchler, J. W.; Kokisch, W.; Smith, P. D. *Struct. Bonding* **1982**, 34, 79−134.

Conclusions

It is concluded that the presently available homonuclear NMR methods allow productive investigation of the active site of ∼40 kDa high-spin ferric heme enzymes, albeit with a more limited information content relative to similar studies on the low-spin, cyanide-inhibited derivatives. Identification of peripheral aromatic contacts allows the determination of the zero-field splitting constant by their characteristic temperature dependence if a homology model is available. It is expected that changes in shifts in resting state peroxidases upon systematic perturbation, such as substrate binding (or point mutation), should be accessible to interpretation in terms of the electronic structure of the heme iron. The limited assignments in HRP^C include key aromatic side chains near pyrrole D which indicate that the substrate binding site of HRP^C and related enzymes can be productively investigated by ^{1}H NMR; such studies are in progress and will be reported elsewhere.[31]

Acknowledgment. The authors thank T. L. Poulos for providing the coordinates of PNP. The authors are indebted to K. Welinder for information on the sequence of the HRP A1 isozyme. This research was supported by a grant from the National Institutes of Health (GM 26226). The NMR instruments were purchased in part from funds provided by the National Institutes of Health (RR-04795) and the National Science Foundation (BBS-88-04739 and DIR-90-16484).

Supporting Information Available: Four figures (2D assignment of 6,7 propionate H_βs in HRP^C; steady-state NOEs from 8-CH_3 in HRP isozymes; TOCSY spectra of Leu 138 analogs in HRP^{A2} and HRP^{A1}; and NOESY spectra for the BHA:HRP^C complex) and three tables (observed chemical shifts for individual heme and axial His resonances for the three HRP isozymes and the effect of BHA binding on HRP^C; δ_{dip}(calc) and δ_{DSS}(calc) for Arg 38, Phe 41, and His 42 based on the homology model; and chemical shifts of heme pocket Phe side chains in HRP^{A1} and HRP^{A2}) (7 pages). See any current masthead page for ordering and Internet access instructions.

JA9642018